JCTC Journal of Chemical Theory and Computation

Article

pubs.acs.org/JCTC

Critical Analysis of Cluster Models and Exchange-Correlation Functionals for Calculating Magnetic Shielding in Molecular Solids

Sean T. Holmes,[†] Robbie J. Iuliucci,[‡] Karl T. Mueller,[§,∥] and Cecil Dybowski*[,†]

[†]Department of Chemistry and Biochemistry, University of Delaware, Newark, Delaware 19716, United States

[‡]Department of Chemistry, Washington and Jefferson College, Washington, Pennsylvania 15301, United States

[§]Department of Chemistry, Pennsylvania State University, University Park, Pennsylvania 16802, United States

[∥]Physical and Computational Sciences Directorate, Pacific Northwest National Laboratory, Richland, Washington 99352, United States

Supporting Information

ABSTRACT: Calculations of the principal components of magnetic-shielding tensors in crystalline solids require the inclusion of the effects of lattice structure on the local electronic environment to obtain significant agreement with experimental NMR measurements. We assess periodic (GIPAW) and GIAO/symmetry-adapted cluster (SAC) models for computing magnetic-shielding tensors by calculations on a test set containing 72 insulating molecular solids, with a total of 393 principal components of chemical-shift tensors from ^{13}C, ^{15}N, ^{19}F, and ^{31}P sites. When clusters are carefully designed to represent the local solid-state environment and when periodic calculations include sufficient variability, both methods predict magnetic-shielding tensors that agree well with experimental chemical-shift values, demonstrating the correspondence of the two computational techniques. At the basis-set limit, we find that the small differences in the computed values have no statistical significance for three of the four nuclides considered. Subsequently, we explore the effects of additional DFT methods available only with the GIAO/cluster approach, particularly the use of hybrid-GGA functionals, meta-GGA functionals, and hybrid meta-GGA functionals that demonstrate improved agreement in calculations on symmetry-adapted clusters. We demonstrate that meta-GGA functionals improve computed NMR parameters over those obtained by GGA functionals in all cases, and that hybrid functionals improve computed results over the respective pure DFT functional for all nuclides except ^{15}N.

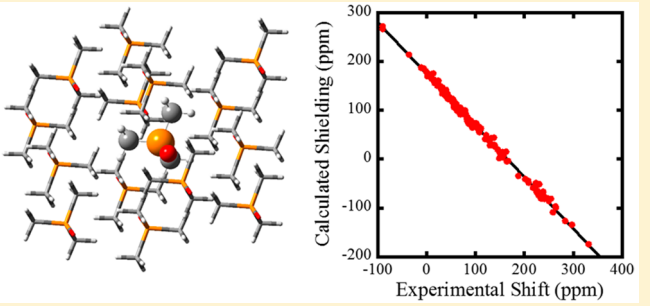

1. INTRODUCTION

The utility of nuclear magnetic resonance (NMR) spectroscopy for molecular analysis results from differences in nuclear transition energies due to variations in the local electronic magnetic field from site to site in a material.[1−3] As such, NMR parameters, specifically magnetic shielding, are sensitive probes of a material's electronic state. Although this connection between electronic state and NMR parameters has long been known,[1] specifying the relationship by detailed calculations has often been a difficult task, particularly for solids. With the advent of numerical techniques using computers to solve quantum-mechanical problems, such as density-functional theory (DFT), predictions of NMR properties have become relatively routine for molecules containing light nuclei such as ^{13}C,[4−7] ^{15}N,[8−10] ^{19}F,[11−24] and ^{31}P.[25−32] However, even with modern techniques, it is often difficult to compare calculations with experiment because there still remain quasi-empirical parameters such as exchange and correlation contributions that are difficult to define in a way universally applicable to all chemical systems.[33−39]

Calculations of NMR parameters for solid materials suffer from several limitations. The first arises from the neglect of intermolecular interactions in the solid state when one uses an isolated-molecule model. The neglected interactions contribute directly and indirectly to the magnetic shielding. The indirect contribution arises from changes in the electron density in the vicinity of the NMR-active nuclei due to interactions with nearby molecules in the lattice that alter the structure of the molecule or the electronic wave function (or both) from its gas-phase structure. In molecular solids, many of the largest deviations in chemical shifts between solid-state and solution-state measurements result from intermolecular hydrogen bonding.[40−44] In addition, lattice forces often distort the structures of molecules in a solid and lower their effective symmetry, resulting in spectra of solid materials that are more complex than those of the same molecule in a dilute gas. Many materials exhibit structural polymorphism, with the material crystallizing in one of several possible space groups, which leads

Received: August 6, 2015

DOI: 10.1021/acs.jctc.5b00752
J. Chem. Theory Comput. XXXX, XXX, XXX−XXX

to a variety of possible local geometries readily distinguishable by NMR spectroscopy. The neglected intermolecular contributions may produce significant differences in the magnetic susceptibility from electronic currents in nearby molecules. For a model to have a useful correspondence to experimental values, these intermolecular effects must be considered explicitly.

The second major limitation involves the level of theory employed in the calculation of NMR parameters to make a problem tractable. Calculated magnetic-shielding parameters frequently have a strong dependence on the model chemistry. The limitation is often a practical one, in which one must trade off accuracy for reasonable computational time. This study focuses on DFT because of the efficiency of the method, which allows systems containing hundreds of atoms to be studied. Compared to post-Hartree−Fock (HF) methods, DFT typically underestimates magnetic-shielding constants.[45,46] This underestimation is often rationalized in terms of a systematic failure in calculating differences between the Kohn−Sham energy levels, leading to overestimations of the paramagnetic contribution to the magnetic shielding. In particular, the relative performance of various exchange-correlation functionals in the prediction of magnetic shielding is of considerable interest.

We discuss two computational schemes to account for the effects of intermolecular interactions on calculations of NMR parameters in insulating molecular solids. The first technique models crystalline solids by using periodic-boundary conditions (PBCs). The second technique employs a finite cluster of molecules to represent a local portion of the solid-state structure.

The gauge-including-projector-augmented-wave (GIPAW) approach of Pickard and Mauri is useful for calculating NMR parameters in periodic systems by expanding the wave function of a crystal in a plane-wave (PW) basis.[47] The size of the basis set is specified by a plane-wave cutoff energy that defines the basis. The GIPAW approach has only been implemented in calculations by pure DFT methods. Hartree−Fock exchange is difficult to implement in plane-wave calculations due to the appearance of a singularity that slows convergence.[48] As such, calculations employing GIPAW are restricted to pure density-functional methods, particularly the local-density approximation (LDA) and the generalized-gradient approximation (GGA).[49] Applications of the GIPAW approach in calculations of NMR parameters have recently been reviewed.[50]

Clusters of molecules have been used as models to determine properties of a solid.[6,11,12,51−58] Recent work from our group has explored the use of clusters in the prediction of magnetic-shielding constants of nuclei such as ^{13}C, ^{207}Pb, and ^{199}Hg.[4,59,60] We have proposed a strategy for systematically designing clusters that reflect the local lattice symmetry to achieve significant agreement with experiment. Of all the possible structures to represent the solid state, symmetry-adapted clusters (SACs) containing the nontranslational-symmetry elements in the space group from the perspective of the central molecule of the cluster provide a geometric model that retains important structural features of the local environment. Clusters without these symmetry requirements may not adequately represent the local environment. For example, building a cluster with only neighboring molecules that participate in hydrogen bonding introduces artificial symmetry constraints. Ensuring proper symmetry usually requires that 11 or more molecules be present in the cluster model. The use of SACs also tends to produce smooth convergence of NMR parameters to a limit with increasing cluster size. The level of theory with which calculations on these symmetry-adapted clusters can be performed is not limited to pure DFT methods, as is the case with GIPAW. Calculations on SACs have been applied to nonperiodic solid or pseudosolid systems such as biomacromolecules,[61] or to systems where the unit cell is very large.

The purpose of this study is, first, to provide a comparison of DFT/GIAO calculations[45,62,63] of magnetic shielding for clusters with calculations using the GIPAW method for a number of different nuclei (^{13}C, ^{15}N, ^{19}F, and ^{31}P) in a variety of different chemical environments. Second, calculations performed using more advanced computational models available with the cluster approach are explored. We show how the use of modern DFT functionals based on hybrid DFT or on the meta-generalized-gradient approximation (meta-GGA) improves agreement between calculation and experiment.

2. COMPUTATIONAL DETAILS

A large series of model compounds was examined. To ensure that sample set did not unnecessarily introduce uncertainty, only compounds that met the following criteria were included: (1) the structure of the material had to be known from high-quality single-crystal diffraction studies, (2) high-resolution measurements of the NMR chemical-shift tensors had to be available for the compound in the same solid phase, and (3) the chemical shifts must have been assigned unambiguously to their respective nuclear sites in the crystalline lattice.

2.1. Materials. Materials were selected to encompass a large variety of chemical environments for ^{13}C, ^{15}N, ^{19}F, and ^{31}P nuclei. Whenever available, neutron-diffraction structures were used to define the structure; otherwise, single-crystal X-ray diffraction provided the structural information.

The database of ^{13}C-containing materials includes naphthalene,[64,65] durene,[66,67] hypoxanthine,[68,69] sucrose,[70,71] oxalic acid,[72,73] oxalic acid dihydrate,[72,74] L-threonine,[75,76] squaric acid,[77,78] cyclopropane,[79,80] ethylene,[81,82] nitromethane,[83,84] acetylene,[85,86] carbon disulfide,[87,88] dimethoxymethane,[89,90] pentaerythritol,[91,92] dimedone,[93,94] norbornadiene,[95,96] and [1.1.1]propellane.[97,98] The database of ^{15}N-containing materials includes adenine trihydrate,[8,99] cytosine,[8,100] guanine monohydrate,[8,101] thymine,[8,102] uracil,[8,103] pyrrole,[9,104] imidazole,[9,105] benzamide,[106,107] benzimidazole,[9,108] nitrobenzene,[109,110] (*E*)-acetophenone oxime,[111,112] pyridine,[9,113] pyridine *N*-oxide,[9,114] acetonitrile,[115,116] 1,4-dicyanobenzene,[117,118] *cis*-azobenzene,[119,120] *trans*-azobenzene,[121,122] and sulfamic acid.[123,124] The database of ^{19}F-containing materials includes fluorobenzene,[125,126] 1,2-difluorobenzene,[125,126] 1,3-difluorobenzene,[125,127] 1,4-difluorobenzene,[125,126] 1,3,5-trifluorobenzene,[125,126] 1,2,4,5-tetrafluorobenzene,[125,128] perfluorobenzene,[129,130] perfluoronaphthalene,[131,132] 2-fluorobenzoic acid,[125,133] 4-fluorobenzoic acid,[125,134] 4,4′-difluorobiphenyl,[135,136] 3-fluorophenol,[125,137] 4-fluorophenol,[125,137] 2-fluorotoluene,[125,138] 3-fluorotoluene,[125,138] 4-fluorotoluene,[125,138] *p*-fluoranil,[125,139] and trichlorofluoromethane.[140,141] The database of ^{31}P-containing materials includes trimethylphosphine oxide,[142,143] triphenylphosphine oxide,[142,144] trichlorophosphine oxide,[145,146] methyldiphenylphosphine oxide,[147,148] trimethylphosphine sulfide,[142,149] tetramethyldiphosphine disulfide,[150,151] tetraethyldiphosphine disulfide,[152] trimethylphosphine selenide,[142,153] urea phosphoric acid,[154,155] methylphos-

DOI: 10.1021/acs.jctc.5b00752
J. Chem. Theory Comput. XXXX, XXX, XXX−XXX

phonic acid,[147,156] 5-phenyl-5H-dibenzophosphole 5-oxide,[157,158] 2,4-bis(methylthio)-1,3-dithia-2,4-diphosphetane-2,4-disulfide,[159,160] 2,4-bis(4-methoxyphenyl)-1,3-dithia-2,4-diphosphetane-2,4-disulfide,[159,161] *cis*-(diphenylimido-2,4,6-tri-*t*-butylphenyl)iminophosphine,[162,163] chloro-(2,4,6-tri-*t*-butylphenyl)iminophosphine,[162,164] tricyclohexylphosphine,[165,166] 1,2,3-triphenylphosphirene,[167,168] and 1,2,2-triphenyl-3,3-bis(trimethylsilyl)phosphirane.[169,170]

Altogether, this database contains 393 principal components of NMR chemical-shift tensors taken from 72 materials. The subset of ^{13}C NMR measurements consists of 177 principal components, of which 96 are sp^3-hybridized, 75 are sp^2-hybridized, and 6 are *sp*-hybridized. The subsets of ^{15}N, ^{19}F, and ^{31}P NMR measurements consist of 99, 60, and 57 principal components, respectively.

2.2. Geometry Optimizations. Refinements of crystal structures obtained from diffraction studies sometimes lead to improvements in calculated NMR parameters.[171,39,154] This consideration is especially important when the material contains hydrogen atoms because the low electron density in the vicinity of these atomic sites leads to relatively large experimental uncertainties in the nuclear coordinates. More accurate methods such as neutron diffraction may have trouble locating the positions of hydrogen atoms in stochastically rotating or librating moieties such as methyl groups, with the result that unrealistically short bond lengths are observed with this technique. Thus, refinement of the positions of light atoms is a necessary prerequisite to calculations in such cases. Studies of fully optimized structures (including heavy atoms) in the presence of a periodic lattice suggest that NMR parameters can be further improved compared to structures where only hydrogen positions are refined.[172] Other studies have found that calculations of NMR parameters obtained from high-quality neutron structures are improved by refinement of hydrogen positions but no significant gain in quality follows from full geometry optimizations.[4]

Because of these considerations, we have chosen to perform fully periodic all-atom plane-wave geometry optimizations on each of the structures of the 72 crystalline materials. Optimizations were performed using fixed lattice parameters because they are generally well-established from experiment. Refined structures produced by the geometry optimizations were used in all subsequent magnetic-shielding calculations.

Geometry optimizations were specifically performed with the CASTEP module of MATERIALS STUDIO 7.0 by Accelrys Software, Inc.[173] The optimizations were carried out at the GGA-PW91/ultrafine level of theory using ultrasoft pseudopotentials (USPP) generated *on the fly*. At the ultrafine level, the plane-wave cutoff varied between 390 and 610 eV, depending on the types of atoms in the lattice. The Brillouin zone was sampled with a *k*-point spacing of 0.07 Å^{-1}. The thresholds for structural convergence were a maximum change in energy of 5×10^{-6} eV per atom, a maximum displacement of 5×10^{-4} Å per atom, and a maximum Cartesian force of 0.01 eV Å^{-1}. For diffraction structures where the hydrogen positions were not published, or where the hydrogen sites were disordered, a preliminary optimization was performed using loosened SCF-convergence criteria to obtain an initial guess for the full geometry optimization.

2.3. Calculations of Magnetic Shielding. Magnetic-shielding constants for the plane-wave-optimized structures were generated using the GIPAW procedure, as implemented in the CASTEP module of MATERIALS STUDIO 7.0. Plane-wave cutoff energies between 200 and 600 eV were examined.[173] Convergence of computed magnetic-shielding constants was verified with respect to plane-wave cutoff energy and *k*-point spacing. The calculations were performed at the GGA-PW91 level of theory. Ultrafine SCF convergence criteria were used in all calculations, independent of the plane-wave cutoff energy. Core orbitals were replaced by USPPs generated *on the fly*.

Magnetic-shielding calculations on symmetry-adapted clusters of molecules that replicated a portion of the crystalline lattice were performed using the GIAO method,[45] as implemented in the GAUSSIAN 09 suite of programs.[174] An example cluster of trimethylphosphine oxide is given in Figure 1. Included in the Supporting Information (Tables S1 and S2)

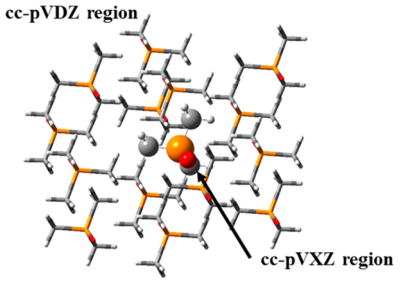

Figure 1. Symmetry-adapted cluster model of trimethylphosphine oxide consisting of 15 molecules in the *C2/m* space group. The central molecule of the cluster (ball-and-stick representation) is given the cc-pVXZ basis set (X = D, T, Q, 5). The peripheral molecules of the cluster (wireframe representation) are given the cc-pVDZ basis set.

are descriptions of the clusters used to replicate the extended lattice structures for the 72 systems in this study. The results presented in sections 3 and 4 were obtained with the GGA-PW91 functional. Results in section 5 were obtained using various DFT methodologies. Our method for calculating magnetic-shielding constants partitioned the cluster into two layers, corresponding to the central molecule and to all peripheral molecules (Figure 1). The low layer (peripheral molecules) was given a less flexible basis set than the high layer (central molecule) to decrease the computational cost. For the central molecule, the basis set cc-pVXZ (X = D, T, Q, 5) was used.[175,176] For the peripheral molecules, cc-pVDZ was used. The effects of this approximation have been discussed previously.[4]

Calculations of magnetic-shielding parameters using the cluster model were also performed using several other DFT functionals. We selected the Perdew–Wang-1991 (GGA-PW91)[177] and Perdew–Burke–Ernzerhof (GGA-PBE)[49] functionals as representative examples of the GGA class. The hybrid equivalents of these are B3PW91[178] and PBE0, respectively.[179] The former (B3PW91) results from the combination of Becke's three-parameter exchange functional[178] with the GGA-PW91 correlation functional. The meta-GGA functional of Tau, Perdew, Staroverov, and Scuseria (TPSS)[180] was used in this analysis with the hybrid analog being labeled TPSSh.[180] The functionals PBE0, TPSS, and TPSSh are related, in that they are modifications of the GGA-PBE functional. To the authors' knowledge, the TPSS and TPSSh functionals have not been studied rigorously for their ability to predict principal components of magnetic-shielding tensors in solids.

DOI: 10.1021/acs.jctc.5b00752
J. Chem. Theory Comput. XXXX, XXX, XXX–XXX

3. INTERMOLECULAR EFFECTS ON MAGNETIC SHIELDING

The importance of intermolecular interactions on computed NMR parameters can be assessed by examining a set of materials where the structure is simplified by considering only a single molecule taken in isolation, as if it were in the gas phase. Such calculations based on isolated-molecule (IM) models ignore all intermolecular contributions to the magnetic shielding. Intermolecular effects on computed NMR parameters can be assessed through calculations using the same plane-wave or atomic-orbital basis set by calculations with and without PBCs, as has been done, for example, in calculations of quadrupolar coupling in titanocene complexes.[181] Here, the results obtained from the IM model are compared with calculations where lattice effects are taken into account using (1) the SAC method or (2) the PBC method. Illustrations of the three computational methodologies are given in Figure 2.

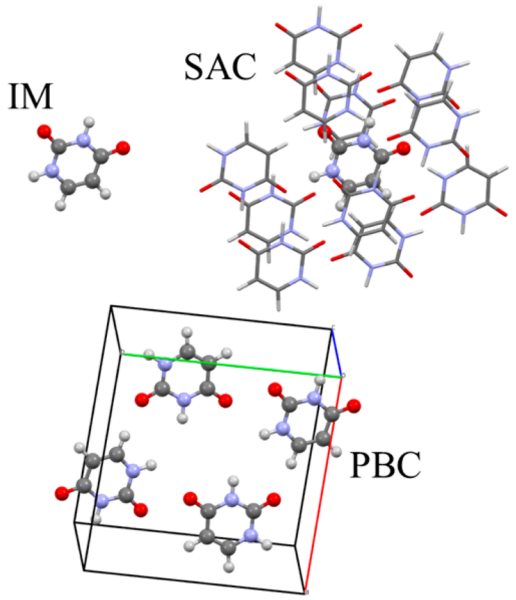

Figure 2. Three computational methodologies used to model the solid-state structure of uracil; isolated-molecule (IM) model, symmetry-adapted-cluster (SAC) model, and periodic-boundary-condition (PBC) model. In the PBC model, the colored lines represent the axes of the unit cell.

We have presented such calculations for a set of ^{13}C-containing materials in previous work[4] and provide similar results in the present study for several ^{15}N-containing materials. All calculations herein were performed using the same plane-wave optimized structures. A summary of the linear-regression parameters for the three computational methodologies is given in Table 1, with computational details provided as a footnote. Correlation plots of calculated principal components of ^{15}N magnetic-shielding tensors versus experimental principal components of ^{15}N chemical-shift tensors illustrating these results are shown in the Supporting Information (Figure S1). The scatter is significantly higher for the IM models (RMSD = 28.5 ppm) than is observed for either the SAC (RMSD = 10.8 ppm) or PBC model (RMSD = 11.4 ppm). Of the 51 magnetic-shielding values, all but eight values are improved over the isolated-molecule model by the SAC model and all but 12 are improved by the PBC model. Of the sites not improved by incorporation of lattice effects, none are significantly worsened.

Table 1. Linear-Regression Parameters for Calculated Principal Components of ^{15}N Magnetic-Shielding Tensors versus Experimental Principal Components of Chemical-Shift Tensors Using Three Computational Models[a−c]

Model	m	$\sigma_{CH_3NO_2}$ (ppm)	RMSD (ppm)[d]
IM	−1.15 ± 0.04	−178 ± 10	28.5
SAC	−1.03 ± 0.01	−155 ± 3	10.8
PBC	−1.06 ± 0.02	−172 ± 4	11.4

[a]GIAO calculations for the IM and SAC models were performed at the PW91/cc-pVTZ level; GIPAW calculations for the PBC model were performed at the PW91/600 eV level. [b]Materials are adenine trihydrate, guanine monohydrate, cytosine, thymine, and uracil with a total of 51 principal components. [c]Linear-regression parameters are given for the correlation line $\sigma_{ii}^{calc} = m\delta_{ii}^{exp} + \sigma_{ref}$, where (σ_{ii}^{calc}) represents the calculated principal components of magnetic-shielding tensors, (δ_{ii}^{exp}) represents experimental principal components of chemical-shift tensors, σ_{ref} is the shielding of the reference compound, CH_3NO_2, and m is the slope of a correlation plot of calculated shielding versus experimental shift. [d]The RMSD is defined by $RMSD = [(N-2)^{-1}\sum_{n=1}^{N}(\delta_{ii}^{calc} - \delta_{ii}^{exp})^2]^{1/2}$. Calculated magnetic shielding is converted to the chemical-shift scale (δ_{ii}^{calc}) using the relationship $\delta_{ii}^{calc} = (\sigma_{ii}^{calc} - \sigma_{ref})/m$.

Furthermore, the slope of −1.15 ± 0.02 in the IM model deviates from unity much more than for the two models that incorporate intermolecular effects (−1.03 ± 0.01 for the SAC model and −1.06 ± 0.02 for the PBC model). There are also significant differences between the extrapolated reference shieldings. Only the IM and SAC models can be compared directly because the PBC model uses a different type of basis set. The reference of the SAC model is predicted to be more shielded than the isolated-molecule model by 23 ± 10 ppm. The similarity in the scatter of the SAC and PBC models suggests that magnetic-shielding values are most sensitive to the immediately surrounding molecules in the crystal lattice and that sufficient agreement with experiment is obtained when representing solid-state effects with a finite cluster (provided that the cluster model satisfies the symmetry requirements of the crystalline space group). It should be emphasized that these calculations were performed on static structures and that the incorporation of dynamic effects on computed NMR parameters may be sizable.[182]

4. COMPARISON OF GIPAW AND GIAO SAC MODELS

Direct comparison of methods based on different computational methodologies is difficult. The GIPAW technique expands the wave function in a plane-wave basis whereas the GIAO method expands the wave function in atom-centered functions. Additionally, each basis is generally truncated, which may lead to errors that affect the quality of the method. The effects of finite basis sets on computed magnetic-shielding parameters have been discussed in numerous articles.[183−190] For example, Kupka et al. have noted that increasing the number of basis functions tends to decrease magnetic-shielding parameters obtained by density-functional calculations.[185,186] One method to deal with this problem involves calculating the magnetic shielding of a suitable reference compound according to both computational procedures and presenting the results as a shift relative to the reference.[191,192] Another approach is to converge both calculations to the basis-set limit. The former method has been employed in calculations of, for example, ^{14}N quadrupolar coupling constants.[193] The latter method has been employed in the present study.

DOI: 10.1021/acs.jctc.5b00752
J. Chem. Theory Comput. XXXX, XXX, XXX−XXX

Table 2. Linear-Regression Parameters Obtained from Correlation Plots between GIPAW Calculated Principal Magnetic-Shielding Values and Experimental Principal Chemical-Shift Values[a,b]

Nucleus	Cutoff Energy (eV)	m	σ_{ref} (ppm)	RMSD (ppm)[c]	Rel. Error[c]
Carbon-13	200	−0.833 ± 0.006	188.3 ± 0.8	8.2	1.94
N = 177	300	−1.009 ± 0.005	175.8 ± 0.6	5.0	1.18
	400	−1.040 ± 0.005	172.5 ± 0.6	4.9	1.16
	500	−1.042 ± 0.005	172.4 ± 0.6	4.9	1.16
	600	−1.043 ± 0.005	172.5 ± 0.6	4.9	1.16
Nitrogen-15	200	−0.61 ± 0.01	41 ± 2	22.8	2.01
N = 99	300	−1.01 ± 0.01	−142 ± 2	17.1	1.51
	400	−1.08 ± 0.01	−175 ± 3	17.3	1.52
	500	−1.09 ± 0.01	−178 ± 3	17.1	1.51
	600	−1.09 ± 0.01	−178 ± 3	17.2	1.51
Fluorine-19	200	−0.71 ± 0.01	301 ± 2	8.1	2.60
N = 60	300	−1.03 ± 0.02	179 ± 2	8.6	2.76
	400	−1.17 ± 0.02	129 ± 3	8.3	2.66
	500	−1.21 ± 0.02	116 ± 3	8.3	2.66
	600	−1.22 ± 0.02	114 ± 3	8.3	2.66
Phosphorus-31	200	−1.05 ± 0.03	284 ± 5	29.9	2.77
N = 57	300	−1.11 ± 0.03	268 ± 5	29.2	2.70
	400	−1.08 ± 0.02	270 ± 4	23.7	2.19
	500	−1.11 ± 0.03	269 ± 5	28.5	2.64
	600	−1.09 ± 0.02	271 ± 4	22.0	2.04

[a]All calculations were performed at the GGA-PW91 level. [b]Linear-regression parameters are given for the correlation line $\sigma_{ii}^{calc} = m\delta_{ii}^{exp} + \sigma_{ref}$, where (σ_{ii}^{calc}) represents the calculated principal components of magnetic-shielding tensors, (δ_{ii}^{exp}) represents experimental principal components of chemical-shift tensors, σ_{ref} is the shielding of the reference compound, and m is the slope of a correlation plot of calculated shielding versus experimental shift. [c]The RMSD is defined by $RMSD = [(N-2)^{-1}\sum_{n=1}^{N}(\delta_{ii}^{calc} - \delta_{ii}^{exp})^2]^{1/2}$. Calculated magnetic shielding is converted to the chemical-shift scale (δ_{ii}^{calc}) using the relationship $\delta_{ii}^{calc} = (\sigma_{ii}^{calc} - \sigma_{ref})/m$. Relative error is the ratio of the RMSD to the experimental chemical-shift range, expressed as a percentage.

Table 3. Linear-Regression Parameters Obtained from Correlation Plots between GIAO SAC Calculated Principal Magnetic-Shielding Values and Experimental Principal Chemical-Shift Values[a,b]

Nucleus	Basis Set	m	σ_{ref} (ppm)	RMSD (ppm)[c]	Rel. Error[c]
Carbon-13	cc-pVDZ	−0.948 ± 0.005	186.4 ± 0.7	5.5	1.30
N = 177	cc-pVTZ	−1.004 ± 0.005	178.2 ± 0.6	5.0	1.18
	cc-pVQZ	−1.031 ± 0.005	175.9 ± 0.6	5.0	1.18
	cc-pV5Z	−1.047 ± 0.005	175.0 ± 0.6	5.0	1.18
	CBS	−1.056 ± 0.005	174.4 ± 0.6	4.9	1.16
Nitrogen-15	cc-pVDZ	−1.01 ± 0.01	−131 ± 2	17.4	1.53
N = 99	cc-pVTZ	−1.05 ± 0.01	−158 ± 2	15.5	1.36
	cc-pVQZ	−1.07 ± 0.01	−168 ± 2	15.4	1.36
	cc-pV5Z	−1.08 ± 0.01	−174 ± 2	15.3	1.35
	CBS	−1.09 ± 0.01	−177 ± 2	15.5	1.36
Fluorine-19	cc-pVDZ	−1.15 ± 0.02	145 ± 3	10.3	3.30
N = 60	cc-pVTZ	−1.18 ± 0.02	132 ± 3	9.6	3.08
	cc-pVQZ	−1.17 ± 0.02	133 ± 3	9.1	2.92
	cc-pV5Z	−1.17 ± 0.02	130 ± 3	9.6	3.08
	CBS	−1.17 ± 0.02	131 ± 3	9.2	2.95
Phosphorus-31	cc-pVDZ	−0.96 ± 0.02	377 ± 4	24.1	2.23
N = 57	cc-pVTZ	−1.02 ± 0.02	318 ± 3	21.3	1.97
	cc-pVQZ	−0.99 ± 0.02	330 ± 3	21.6	2.00
	cc-pV5Z	−1.09 ± 0.02	279 ± 3	20.6	1.91
	CBS	−1.09 ± 0.02	269 ± 3	21.1	1.95

[a]All calculations were performed at the GGA-PW91 level. [b]Linear-regression parameters are given for the correlation line $\sigma_{ii}^{calc} = m\delta_{ii}^{exp} + \sigma_{ref}$, where (σ_{ii}^{calc}) represents the calculated principal components of magnetic-shielding tensors, (δ_{ii}^{exp}) represents experimental principal components of chemical-shift tensors, σ_{ref} is the shielding of the reference compound, and m is the slope of a correlation plot of calculated shielding versus experimental shift. [c]The RMSD is defined by $RMSD = [(N-2)^{-1}\sum_{n=1}^{N}(\delta_{ii}^{calc} - \delta_{ii}^{exp})^2]^{1/2}$. Calculated magnetic shielding is converted to the chemical-shift scale (δ_{ii}^{calc}) using the relationship $\delta_{ii}^{calc} = (\sigma_{ii}^{calc} - \sigma_{ref})/m$. Relative error is the ratio of the RMSD to the experimental chemical-shift range, expressed as a percentage.

Using a class of basis sets such as cc-pVXZ allows the basis-set limit to be reached in a systematic manner for the GIAO approach. GIPAW and GIAO/SAC methodologies can be compared meaningfully using NMR parameters extrapolated to

DOI: 10.1021/acs.jctc.5b00752
J. Chem. Theory Comput. XXXX, XXX, XXX−XXX

the basis-set limit. Calculations were performed by incrementally increasing the plane-wave cutoff energy (PBC method) or the number of Cartesian basis functions (SAC method), while maintaining the SCF convergence criteria. For the PBC calculations, the basis-set limit seems to be approached for a cutoff energy of 600 eV. Calculations on several systems using higher cutoff energies did not substantially alter the computed values found using a cutoff energy of 600 eV. For SACs, the basis-set limit is given by an extrapolated value obtained by modeling the change in magnetic-shielding with basis-set size.[185,186]

Linear-regression parameters for the correlation between calculated principal components of magnetic-shielding tensors and experimental principal components of chemical-shift tensors are presented in Table 2 for the PBC method and in Table 3 for the SAC method. An evaluation of the data presented in these tables reveals several important trends that are generally consistent among the nuclei. For the first-row nuclei (^{13}C, ^{15}N, ^{19}F), individual principal components exponentially approach the basis-set limit. For ^{31}P, individual principal components approach the basis-set limit either exponentially or in a damped-oscillatory fashion. Importantly, both the PBC and SAC methods approach the same reference shielding within experimental uncertainty at the basis-set limit for all nuclei except ^{19}F. The linear-regression parameters vary in a manner that reflects the changes in the individual principal components. Each increase in the number of basis functions leads to deshielding of the reference compound.

Plots comparing calculated principal components of magnetic-shielding tensors with experimental principal components of chemical-shift tensors are shown in Figure 3. These correlation plots demonstrate the equivalence of GIPAW and GIAO for all nuclides but ^{19}F. At the basis-set limit, in every case, the slope of the correlation line has a magnitude greater than unity, indicating that calculations performed at the GGA-PW91 level of theory overestimate differences in chemical shifts between nuclear sites and overestimate the anisotropies of individual sites. It is notable that the data set yielding a slope closest to −1 is the set of ^{13}C shifts, with the GIPAW method predicting a slope of −1.043 ± 0.005 and the GIAO method predicting a slope of −1.056 ± 0.005. ^{15}N yields a slope of −1.09 ± 0.01 and ^{31}P yields a slope of −1.09 ± 0.02 for both computational methodologies. The slope of the ^{19}F linear-regression line depends on the computational methodology, with the GIPAW method having a slope of −1.22 ± 0.02 and the GIAO method having a slope of −1.17 ± 0.02.

For calculations of ^{15}N and ^{31}P shieldings, there is no difference in linear-regression parameters between the two computational methodologies. Similarly, the differences observed for ^{13}C are small, with a difference in σ_{TMS} of 1.9 ± 0.8 ppm and a difference in slope of 0.013 ± 0.007. For ^{19}F, the reference shielding σ_{CFCl_3} for the GIAO value is shielded relative to the GIPAW value by 17 ± 4 ppm. In addition, the slopes of the lines differ by 0.05 ± 0.03, with the GIAO method yielding a result closer to unity. Statistical analysis using the *T*-test was used to determine whether these differences observed in the trend lines represent a significant difference between the two computational models. This question is equivalent to asking if the computed results from the cluster method can be modeled using the trend line obtained by analyzing the GIPAW results. This can be evaluated by tabulating the RMSDs according to the two modeling techniques and defining a threshold for

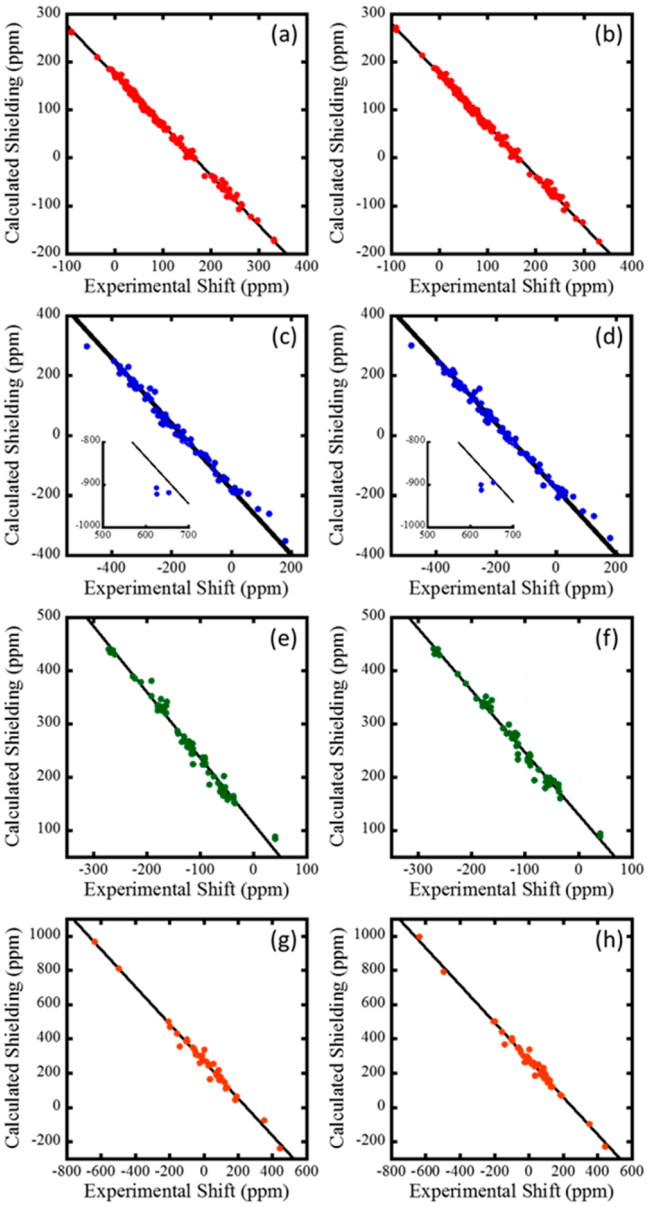

Figure 3. Calculated principal components of magnetic-shielding tensors versus experimental principal components of chemical-shift tensors. Chemical shifts are reported with respect to TMS for ^{13}C (red), CH_3NO_2 for ^{15}N (blue), $CFCl_3$ for ^{19}F (green), and 85% H_3PO_4 for ^{31}P (orange). Values are computed using the periodic GIPAW model (left column) and the GIAO SAC model (right column). For ^{13}C calculations, the correlation lines are given by $\sigma_{ii}^{GIPAW} = (-1.043 \pm 0.005)\delta_{ii} + (172.5 \pm 0.6)$ ppm in (a) and by $\sigma_{ii}^{GIAO} = (-1.056 \pm 0.005)\delta_{ii} + (174.4 \pm 0.6)$ ppm in (b). For ^{15}N calculations, the correlation lines are given by $\sigma_{ii}^{GIPAW} = (-1.09 \pm 0.01)\delta_{ii} + (-178 \pm 3)$ ppm in (c) and by $\sigma_{ii}^{GIAO} = (-1.09 \pm 0.01)\delta_{ii} + (-179 \pm 3)$ ppm in (d). For ^{19}F, the correlation lines are given by $\sigma_{ii}^{GIPAW} = (-1.22 \pm 0.02)\delta_{ii} + (114 \pm 3)$ ppm in (e) and by $\sigma_{ii}^{GIAO} = (-1.17 \pm 0.02)\delta_{ii} + (131 \pm 3)$ ppm in (f). For ^{31}P, the correlation lines are given by $\sigma_{ii}^{GIPAW} = (-1.09 \pm 0.02)\delta_{ii} + (270 \pm 4)$ ppm in (g) and by $\sigma_{ii}^{GIAO} = (-1.09 \pm 0.02)\delta_{ii} + (269 \pm 3)$ ppm in (h). The insets in (c) and (d) show calculations for σ_{33} principal components of azo nitrogens.

significance. These results are shown in Table 4. At the 95% level, there is no significant difference between the computed magnetic-shielding parameters for ^{13}C, ^{15}N, or ^{31}P. However, there is a statistical difference between the GIPAW and GIAO cluster methods for computed magnetic shielding of ^{19}F sites.

DOI: 10.1021/acs.jctc.5b00752
J. Chem. Theory Comput. XXXX, XXX, XXX−XXX

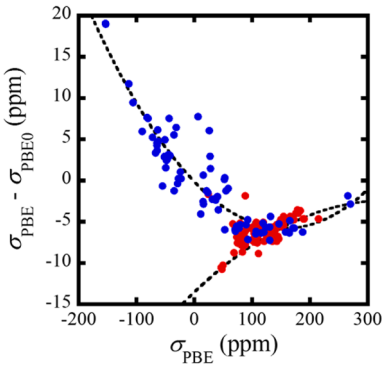

Figure 4. Difference between GGA-PBE- and PBE0-calculated ^{13}C principal chemical-shielding values for sp^3-hybridized (red) and sp^2- and sp-hybridized (blue) sites. The trend lines are meant to guide the eye.

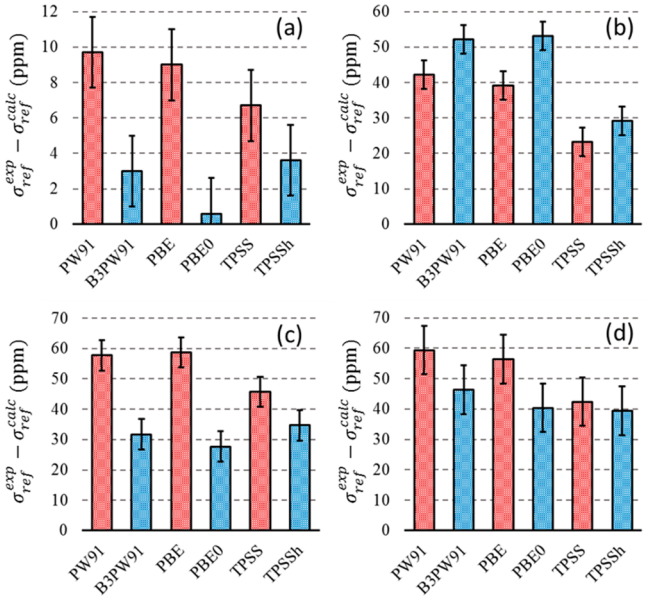

Figure 5. Deviation of the extrapolated magnetic shielding of the reference compound obtained with least-squares analyses for various DFT functionals from the accepted literature value. Results are shown for ^{13}C (a), ^{15}N (b), ^{19}F (c), and ^{31}P (d). The reference compounds and literature shielding values are TMS at 184.1 ppm (^{13}C),[206] CH_3NO_2 at −135.8 ppm (^{15}N),[207] $CFCl_3$ at 188.7 ppm (^{19}F),[208] and 85% H_3PO_4 at 328.4 ppm (^{31}P).[209] A finite-basis-set correction was applied to each calculated value by subtracting 3.8 ppm (^{13}C), 19 ppm (^{15}N), 1 ppm (^{19}F), and 48 ppm (^{31}P) from calculated values of σ_{ref}. The error bars represent both the uncertainty in the calculated and experimental values and the basis-set correction. Pure DFT functionals are shown in red, and hybrid functionals are shown in blue.

Table 4. *T*-Test Statistics for Assessing Differences between the GIPAW and GIAO/Cluster Methodologies for Computing Magnetic-Shielding Parameters[a]

Nucleus	*N*	ΔRMSD (ppm)	RMSD Cutoff (ppm)
Carbon-13	177	0.08	0.10
Nitrogen-15	99	0.03	0.29
Fluorine-19	60	4.68	2.23
Phosphorus-31	57	0.04	0.47

[a]Differences between the computational methodologies are significant if ΔRMSD is greater than the RMSD cutoff.

To explore this deviation further, the ^{19}F magnetic-shielding constants were calculated using Jensen's segmented polarization-consistent basis set pcSseg-3, which is optimized for calculations of magnetic-shielding constants.[194] Similar results were obtained using both the correlation-consistent (cc-pVTZ) and polarization-consistent (pcSseg-3) basis sets, with the equations of the correlations lines given by

$$\sigma_{ii}^{cc\text{-}pVTZ} = (-1.18 \pm 0.02)\delta_{ii}^{calc} + (132 \pm 3)\ \text{ppm} \quad (1)$$

$$\sigma_{ii}^{pcSseg\text{-}3} = (-1.18 \pm 0.02)\delta_{ii}^{calc} + (129 \pm 3)\ \text{ppm} \quad (2)$$

Augmented basis sets such as aug-cc-pVTZ and aug-pcSseg-3 typically altered ^{19}F magnetic shielding no more than 1 ppm.

5. EXAMINATION OF EXCHANGE-CORRELATION FUNCTIONALS

Computed NMR parameters display a strong dependence on the model chemistry used in the calculation. Most studies that have explored level-of-theory effects on NMR parameters have examined the effects on the isotropic shielding of nuclei in gas-phase molecules. Highly accurate benchmark magnetic-shielding constants from coupled-cluster calculations have been presented for the four nuclei in this study (^{13}C, ^{15}N, ^{19}F, and ^{31}P).[7,10,18] NMR parameters obtained from various DFT methods have been benchmarked against values computed using *ab initio* methods such as Hartree−Fock or MP2[45,46,195] and against other DFT methods.[24,196−201]

Considering only the isotropic value of the magnetic-shielding tensor ignores the significant role that the choice of functional may have on the computed anisotropy and asymmetry of the magnetic-shielding tensor. Analyses involving comparisons of the principal components of magnetic-shielding tensors are comparatively rare. A study by Sefzik et al. correlated computed principal components of ^{13}C magnetic-shielding tensors obtained from IM models with experimental values obtained in solids.[202] Several studies have used the GIPAW method to compare various GGA functionals.[19,172,203−205] None of these studies found a significant difference between the GGA functionals.

We have previously explored hybrid DFT functionals for calculating principal components of ^{13}C magnetic-shielding tensors.[4] Another recent study has also suggested that hybrid functionals improve the agreement with experimental ^{13}C chemical shift over GGA functionals.[6] This result has not been generalized to other nuclei, although a preliminary analysis has found that hybrid functionals can alleviate certain systematic problems associated with calculations of ^{207}Pb magnetic shielding.[60]

We demonstrate that the SAC model can be employed in a systematic investigation of differences in computed principal components of magnetic-shielding tensors determined with different classes of DFT functionals. Linear-regression parameters obtained from calculations using six functionals (GGA-PW91, B3PW91, GGA-PBE, PBE0, meta-GGA-TPSS, and TPSSh) are summarized in Table 5.

5.1. Discussion of ^{13}C Results. The ^{13}C results in Table 5 demonstrate that, for this nucleus, the GGA functionals (PW91 and PBE) are outperformed by every other class of functional studied, as indicated by the RMSDs of the various data sets. Using the scatter as the sole criterion for goodness-of-fit, the hybrid functionals seem to outperform the others.

DOI: 10.1021/acs.jctc.5b00752
J. Chem. Theory Comput. XXXX, XXX, XXX−XXX

Table 5. Linear-Regression Parameters from Correlations between Calculated Principal Components of Magnetic-Shielding Tensors and Experimental Chemical-Shift Principal Components Using the Symmetry-Adapted-Cluster Approach[a,b]

Nucleus	Method	m	σ_{ref} (ppm)	RMSD (ppm)[c]	Rel. Error[c]
Carbon-13	PW91	−1.004 ± 0.005	178.2 ± 0.6	5.0	1.18
N = 177	B3PW91	−1.045 ± 0.005	184.9 ± 0.6	4.6	1.09
	PBE	−1.001 ± 0.005	178.9 ± 0.6	5.0	1.18
	PBE0	−1.050 ± 0.005	187.3 ± 0.6	4.7	1.11
	TPSS	−0.982 ± 0.005	181.2 ± 0.6	4.9	1.16
	TPSSh	−1.004 ± 0.004	184.3 ± 0.6	4.7	1.11
Nitrogen-15	PW91	−1.05 ± 0.01	−158 ± 2	15.5	1.36
N = 99	B3PW91	−1.11 ± 0.01	−168 ± 2	16.2	1.43
	PBE	−1.04 ± 0.01	−156 ± 2	15.8	1.39
	PBE0	−1.12 ± 0.01	−170 ± 2	16.7	1.47
	TPSS	−0.995 ± 0.007	−140 ± 2	13.5	1.19
	TPSSh	−1.026 ± 0.007	−145 ± 2	13.5	1.19
Fluorine-19	PW91	−1.18 ± 0.02	132 ± 3	9.6	3.08
N = 60	B3PW91	−1.11 ± 0.02	158 ± 3	10.2	3.27
	PBE	−1.18 ± 0.02	131 ± 3	9.6	3.08
	PBE0	−1.10 ± 0.02	162 ± 3	10.6	3.40
	TPSS	−1.13 ± 0.02	145 ± 3	10.5	3.37
	TPSSh	−1.11 ± 0.02	156 ± 3	10.5	3.37
Phosphorus-31	PW91	−1.02 ± 0.02	318 ± 3	21.3	1.97
N = 57	B3PW91	−1.03 ± 0.02	331 ± 3	20.4	1.89
	PBE	−1.02 ± 0.02	322 ± 3	20.9	1.93
	PBE0	−1.03 ± 0.02	339 ± 3	21.0	1.94
	TPSS	−0.99 ± 0.02	335 ± 3	21.7	2.01
	TPSSh	−0.99 ± 0.02	339 ± 3	22.2	2.05

[a]Calculated values were obtained using the cc-pVTZ basis set. [b]Linear-regression parameters are given for the correlation line $\sigma_{ii}^{calc} = m\delta_{ii}^{exp} + \sigma_{ref}$, where (σ_{ii}^{calc}) represents the calculated principal components of magnetic-shielding tensors, (δ_{ii}^{exp}) represents experimental principal components of chemical-shift tensors, σ_{ref} is the shielding of the reference compound, and m is the slope of a correlation plot of calculated shielding versus experimental shift. [c]The RMSD is defined by RMSD = $[(N-2)^{-1}\sum_{n=1}^{N}(\delta_{ii}^{calc} - \delta_{ii}^{exp})^2]^{1/2}$. Calculated magnetic shielding is converted to the chemical-shift scale (δ_{ii}^{calc}) using the relationship $\delta_{ii}^{calc} = (\sigma_{ii}^{calc} - \sigma_{ref})/m$. Relative error is the ratio of the RMSD to the experimental chemical-shift range, expressed as a percentage.

A significant difficulty in the analysis of carbon data arises because different carbon species tend to group into distinct subpopulations on the correlation plot. Several studies have found that the correlation line between calculated magnetic shielding and experimental chemical shift for distinct carbon species can differ by a substantial amount.[202,5] The differences appear to be more pronounced when the materials under consideration are constrained to a well-defined class of compounds such as carbohydrates or aromatic hydrocarbons.[202] Our previous work has suggested that hybrid functionals remove the systematic differences between carbon subpopulations, resulting in a unique trend line which can successfully model all carbon species. As above, statistical analysis was used to determine if the two classes of carbon species (sp^3 and sp^2/sp) represent statistically significant subpopulations at the 95% confidence level (Table 6). We find that when using pure DFT functionals (GGA-PW91, GGA-PBE, meta-GGA-TPSS), the two carbon species represent distinct subpopulations, whereas the hybrid functionals (B3PW91, PBE0, TPSSh) do not result in distinct subpopulations.

The two carbon subpopulations can be visualized in the systematic differences between calculated magnetic-shielding parameters using a GGA functional and a hybrid functional. Figure 4 shows differences between principal magnetic-shielding values obtained from the GGA-PBE and PBE0 functionals for carbons in different hybridization. Carbons at sp^3 sites behave differently from sp^2 and sp sites. For the sp^3-hybridized sites, where the electron density is much more homogeneous around the nuclear site, the added flexibility of the hybrid functional has a lesser effect than for the sp^2- and sp-hybridized sites, where the electron density, and therefore the corresponding current density, varies substantially with orientation. In Figure 4 one sees that σ_{11} and σ_{22} components for the sp^2- and sp-hybridized sites tend to be more affected by the use of the hybrid functionals than the GGA functionals, whereas there is a lesser difference for σ_{33}.

Table 6. Linear-Regression Parameters and T-Test Statistics for Assessing Differences between sp^3- and sp^2/sp-Hybridized Carbon Subpopulations[a]

	sp^3		sp^2/sp		
Method	m	σ_{ref} (ppm)	m	σ_{ref} (ppm)	ΔRMSD (ppm)
PW91	−1.049	180.2	−1.005	178.9	0.7
B3PW91	−1.031	184.0	−1.046	184.9	0.1
PBE	−1.048	181.0	−1.001	179.4	0.7
PBE0	−1.025	185.9	−1.050	186.9	0.1
TPSS	−1.018	182.6	−0.985	182.2	0.6
TPSSh	−1.012	184.3	−1.006	184.9	0.1

[a]Differences in the best-fit lines between sp^3 and sp^2 carbon species are statistically significant if the ΔRMSD is greater than 0.2 ppm.

Differences between the experimental value for the shielding of TMS (184.1 ppm)[206] and the extrapolated values (as reported in Table 5) are shown in Figure 5(a) for the six functionals considered in the present work. Because the

DOI: 10.1021/acs.jctc.5b00752
J. Chem. Theory Comput. XXXX, XXX, XXX−XXX

absolute shielding for TMS is predicted to be more deshielded when increasing the number of basis functions, we have applied a finite basis-set correction to the reference shieldings of −3.8 ± 0.8 ppm, based on the difference between the reference values for the cc-pVTZ basis set and the basis-set limit. The results illustrate that the hybrid functionals more closely predict the reference shielding than do the pure DFT functionals. The best results were obtained with PBE0. The meta-GGA functional (TPSS) results in an improvement in the reference value, intermediate between the GGA functionals and the hybrid functionals.

5.2. Discussion of ^{15}N results. In calculation of ^{15}N shielding, the RMSDs range between 16.8 ppm (PBE0) and 13.6 ppm (TPSSh), as shown in Table 5. Using the scatter about the best-fit line as the criterion for judging the functionals, the best class of functionals appears to be the meta-GGAs (TPSS and TPSSh), whereas the worst class of functionals is the hybrid GGAs (B3PW91 and PBE0). The meta-GGA functionals yield slopes closest to unity, ranging between −0.995 ± 0.007 (TPSS) and −1.027 ± 0.007 (TPSSh). These values represent an improvement over the predicted slope of −1.04 ± 0.01 for GGA-PBE. The hybrid functionals have slopes ranging between −1.11 ± 0.01 (B3PW91) and −1.12 ± 0.01 (PBE0), as compared to the meta-GGA functionals.

The use of GGA and hybrid-GGA functionals in ^{15}N calculations differs from their use with other nuclei in one significant way: whereas the reference values of the other nuclei (^{13}C, ^{19}F, ^{31}P) are predicted to be more *shielded* (relative to the pure DFT functional) when using hybrid functionals, for ^{15}N the use of hybrid functionals yields reference values that are *deshielded*. In the most significant case, the reference shielding for the GGA-PBE functional is −156 ± 2 ppm and the reference for the PBE0 functional is −170 ± 2 ppm. Figure 5(b) displays differences between the predicted intercept and the literature value of −135.8 ppm for the bare nucleus.[207] As in the case of carbon, a finite-basis-set correction of 19 ± 3 ppm has been introduced. Interestingly, meta-GGA functionals are the closest to the literature value. In each case, using a hybrid functional increases the deviation from the literature value than does the pure DFT value.

Figure 6(a) shows the differences in magnetic shielding between the GGA-PBE functional and the PBE0 functional versus the GGA-PBE shielding. This plot illustrates that the quantity $\sigma_{PBE} - \sigma_{PBE0}$ varies significantly across the range of computed magnetic shieldings. Similarly, Figure 6(b) shows the differences in magnetic shielding between the GGA-PBE functional and the meta-GGA-TPSS functional versus the GGA-PBE shielding. The most significant changes are seen in the calculations of σ_{33} for the ^{15}N nuclei of azide groups, located around −900 ppm at the GGA-PBE level. In the PBE0 calculations, the azide σ_{33} is predicted to be *deshielded* relative to the GGA-PBE calculations by 67−84 ppm, whereas the TPSS calculation predicts these sites to be *shielded* relative to the PBE calculation by 65−77 ppm. As indicated in Figure 3, these points deviate from the predicted trend line by a sizable amount at the GGA level. This deviation is worsened when using hybrid GGA functionals. When using the TPSS functional, the points fall along the same line predicted by the other calculations, suggesting that meta-GGA functionals improve calculations of highly correlated systems such as those containing nitrogen−nitrogen double bonds.

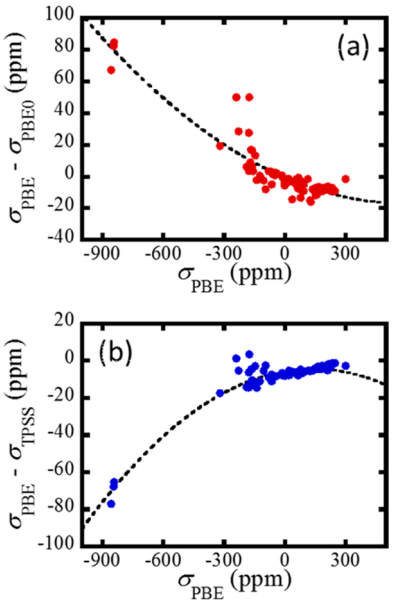

Figure 6. (a) Differences in computed shielding between the GGA-PBE functional and the hybrid GGA-PBE0 functional. (b) Differences in computed shielding between the GGA-PBE functional and the meta-GGA-TPSS functional.

5.3. Discussion of ^{19}F results. A frequent feature of computed ^{19}F NMR parameters is that they are predicted less reliably than are the NMR parameters of other light nuclei, as is indicated by the substantial deviation in the slope from unity, signifying that the errors arise from a systematic flaw in the calculations. At the basis-set limit, the GIPAW method predicts a slope of −1.22 ± 0.02 at the PW91 level. Comparable systematic errors have been reported in calculations performed at similar levels of theory,[24,23] where it has been shown that altering the computed band gap by applying potentials to certain molecular orbitals corrects systematic flaws in the calculations. Such a correction is empirical and the size of the potential is dependent on the system.

Considering the results in Table 5, the GGA and meta-GGA functionals overestimate the slope substantially. Hybrid functionals decrease the slope, with the best result of −1.10 ± 0.02 obtained from the B3PW91 functional, and reduce the magnitude of the discrepancy so that the slope is within the range of values computed for the other nuclei. This finding suggests that large changes in the magnetic shielding can be induced by the method for calculating the exchange energy. There are two lines of evidence that suggest that the errors in the calculated values are related to the exchange functional. Moving from the GGA-PBE functional (0% HF exchange) to the PBE0 functional (25% HF exchange), the slope of the correlation line is changed from −1.18 ± 0.02 to −1.10 ± 0.02, suggesting that increasing the proportion of exact exchange to around 50% would eliminate deviations in the slope. Jameson et al. have proposed an absolute reference for ^{19}F where the shielding of $CFCl_3$ is 188.7 ppm.[208] Changing from the PBE functional to the PBE0 functional changes the extrapolated reference shielding from 131 ± 3 ppm at the PBE level to 162 ± 3 at the PBE0 level, consistent with an ideal functional that uses approximately 50% HF exchange. See Figure 5(c).

5.4. Discussion of ^{31}P results. The ^{31}P results in Table 5 reveal only small deviations between the different classes of functionals for calculations of ^{31}P magnetic shielding. In

DOI: 10.1021/acs.jctc.5b00752
J. Chem. Theory Comput. XXXX, XXX, XXX−XXX

particular, the slopes of the best-fit lines are the same, to within experimental error. The largest deviations between functionals are seen in the reference shieldings. Jameson et al. suggest a reference shielding for H_3PO_4 of 328.4 ppm.[209] The results, shown in Figure 5(d), mirror those obtained for ^{13}C and ^{19}F. As with those nuclei, use of a hybrid functional always results in an improvement over the pure DFT functional. In addition, improvement is found for the meta-GGA-TPSS functional over the GGA functionals.

6. CONCLUSIONS

Consideration of intermolecular effects is essential when calculating NMR parameters for crystalline materials. The periodic GIPAW method, for example, accounts for intermolecular interactions that are not predicted by calculations on isolated molecules (especially in systems containing networks of intermolecular hydrogen bonds). The use of symmetry-adapted-cluster (SAC) models yields similar results to those obtained using GIPAW, showing the importance of inclusion of intermolecular effects in predicting magnetic shielding in solids.

The use of the GIPAW and GIAO/SAC methods for calculating the magnetic shielding of ^{13}C, ^{15}N, ^{19}F, and ^{31}P nuclides in insulating molecular solids demonstrates that one may systematically model a wide variety of solid-state environments with either method, if one uses a sufficiently large basis. This result is demonstrated on a database consisting of 72 crystalline materials with a total of 131 unique NMR-active lattice sites. Computed magnetic shieldings extrapolated to the basis-set limit show that the two methods predict correlation lines that show no statistical difference at the 95% level for all nuclei except ^{19}F. In the case of ^{19}F, the correlation between experimental chemical shifts and calculated magnetic shielding yields a slope closer to unity with the SAC method.

The effects of various model chemistries on computed magnetic shielding have been assessed using the SAC model. Six exchange-correlation functionals have been examined, representing the GGA, hybrid GGA, meta-GGA, and hybrid meta-GGA classes. There is essentially no difference in computed magnetic shielding between GGA functionals (PW91 and PBE) for any of the nuclides studied here. Hybrid GGA functionals yield results that are often quite different from those determined with pure DFT functionals. For ^{13}C, ^{19}F, and ^{31}P, the additional flexibility of using hybrid functionals leads to improvement of the predicted magnetic shielding with values determined on established absolute scales. In particular, for ^{19}F magnetic shielding, the use of hybrid functionals substantially decreases the slope of the correlation between calculated shielding and experimental shift from −1.18 when using GGAs to −1.11. For ^{19}F, we suggest that increasing the proportion of HF exchange beyond the standard 25% may further improve agreement with experiment, although this result needs to be explored in more detail. Calculations of ^{15}N magnetic shielding, in contrast to the other nuclei, appear to be worsened by the admixture of exact exchange, as indicated by a slope that is further from unity and a reference shielding that differs more substantially from established scales. The use of the meta-GGA-TPSS functional leads to improvement over the GGA functionals for all four nuclei.

It is also noteworthy that ^{13}C magnetic-shielding parameters obtained by pure DFT methods can be grouped into distinct subpopulations based on the hybridization of the carbon site. However, use of hybrid DFT functionals does not lead to distinct subpopulations, allowing all carbon species to be described with a single set of linear-regression parameters.

■ ASSOCIATED CONTENT

Supporting Information

The Supporting Information is available free of charge on the ACS Publications website at DOI: 10.1021/acs.jctc.5b00752.

Composition of symmetry-adapted clusters, correlation plots from section 3 (PDF)

■ AUTHOR INFORMATION

Corresponding Author

*E-mail: dybowski@udel.edu.

Funding

C.D. acknowledges the support of the National Science Foundation under Grant CHE-0956006, and K.T.M. acknowledges the support of the National Science Foundation under Grant CHE-1213451.

Notes

The authors declare no competing financial interest.

■ ACKNOWLEDGMENTS

Helpful discussions with Mr. Fahri Alkan are acknowledged.

■ REFERENCES

(1) Ramsey, N. F. *Phys. Rev.* **1950**, *78*, 699.
(2) Slichter, C. P. *Principles of Magnetic Resonance*, 3rd ed.; Springer-Verlag: Heidelberg, 1992.
(3) Pople, J. A.; Schneider, W. G.; Bernstein, H. J. *High-Resolution Nuclear Magnetic Resonance*; McGraw-Hill: New York, 1959.
(4) Holmes, S. T.; Iuliucci, R. J.; Mueller, K. T.; Dybowski, C. *J. Chem. Phys.* **2014**, *141*, 164121.
(5) Johnston, J. C.; Iuliucci, R. J.; Facelli, J. C.; Fitzgerald, G.; Mueller, K. T. *J. Chem. Phys.* **2009**, *131*, 144503/1.
(6) Hartman, J. D.; Monaco, S.; Schatschneider, B.; Beran, G. J. O. *J. Chem. Phys.* **2015**, *143*, 102809.
(7) Auer, A. A.; Gauss, J.; Stanton, J. F. *J. Chem. Phys.* **2003**, *118*, 10407.
(8) Hu, J. Z.; Facelli, J. C.; Alderman, D. W.; Pugmire, R. J.; Grant, D. M. *J. Am. Chem. Soc.* **1998**, *120*, 9863.
(9) Solum, M. S.; Altman, K. L.; Strohmeier, M.; Berges, D. A.; Zhang, Y.; Facelli, J. C.; Pugmire, R. J.; Grant, D. M. *J. Am. Chem. Soc.* **1997**, *119*, 9804.
(10) Prochnow, E.; Auer, A. A. *J. Chem. Phys.* **2010**, *132*, 064109.
(11) Cai, S.-H.; Chen, Z.; Wan, H.-L. *J. Phys. Chem. A* **2002**, *106*, 1060.
(12) Body, M.; Silly, G.; Legein, C.; Buzare, J.-Y. *J. Phys. Chem. B* **2005**, *109*, 10270.
(13) Chan, J. C. C.; Eckert, H. *J. Mol. Struct.: THEOCHEM* **2001**, *535*, 1.
(14) Ebrahimi, H. P.; Tafazzoli, M. *Concepts Magn. Reson., Part A* **2013**, *42*, 140.
(15) Saielli, G.; Bini, R.; Bagno, A. *Theor. Chem. Acc.* **2012**, *131*, 1140.
(16) Zheng, A. M.; Liu, S. B.; Deng, F. *J. Phys. Chem. C* **2009**, *113*, 15018.
(17) Ebrahimi, H. P.; Tafazzoli, M. *Concepts Magn. Reson., Part A* **2012**, *40A*, 192.
(18) Harding, M. E.; Lenhart, M.; Auer, A. A.; Gauss, J. *J. Chem. Phys.* **2008**, *128*, 244111.
(19) Robbins, A. J.; Ng, W. T. K.; Jochym, D.; Keal, T. W.; Clark, S. J.; Tozer, D. J.; Hodgkinson, P. *Phys. Chem. Chem. Phys.* **2007**, *9*, 2389.
(20) de Dios, A. C.; Oldfield, E. *J. Am. Chem. Soc.* **1994**, *116*, 7453.
(21) Sanders, L. K.; Oldfield, E. *J. Phys. Chem. A* **2001**, *105*, 8098.
(22) Sternberg, U.; Klipfel, M.; Grage, S. L.; Witter, R.; Ulrich, A. S. *Phys. Chem. Chem. Phys.* **2009**, *11*, 7048.

DOI: 10.1021/acs.jctc.5b00752
J. Chem. Theory Comput. XXXX, XXX, XXX−XXX

(23) Sadoc, A.; Body, M.; Legein, C.; Biswal, M.; Fayon, F.; Rocquefelte, X.; Boucher, F. *Phys. Chem. Chem. Phys.* **2011**, *13*, 18539.
(24) Laskowski, R.; Blaha, P.; Tran, F. *Phys. Rev. B: Condens. Matter Mater. Phys.* **2013**, *87*, 195130.
(25) Chesnut, D. B.; Rusiloski, B. E. *Chem. Phys.* **1991**, *157*, 105.
(26) Tong, J.; Liu, S.; Zhang, S.; Li, S. Z. *Spectrochim. Acta, Part A* **2007**, *67*, 837.
(27) van Wullen, C. *Phys. Chem. Chem. Phys.* **2000**, *2*, 2137.
(28) Latypov, S. K.; Polyancev, F. M.; Yakhvarov, D. G.; Sinyashin, O. G. *Phys. Chem. Chem. Phys.* **2015**, *17*, 6976.
(29) Maryasin, B.; Zipse, H. *Phys. Chem. Chem. Phys.* **2011**, *13*, 5150.
(30) Pourpoint, F.; Kolassiba, A.; Gervais, C.; Azais, T.; Bonhomme-Coury, L.; Bonhomme, C.; Mauri, F. *Chem. Mater.* **2007**, *19*, 6367.
(31) Vasconcelos, F.; Cristol, S.; Paul, J. F.; Montagne, L.; Mauri, F.; Delevoye, L. *Magn. Reson. Chem.* **2010**, *48*, S142.
(32) Fedorov, S. V.; Rusakov, Y. Y.; Krivdin, L. B. *Magn. Reson. Chem.* **2014**, *52*, 699.
(33) Orendt, A. M.; Facelli, J. C. *Annu. Rep. NMR Spectrosc.* **2007**, *62*, 115.
(34) Facelli, J. C. *Prog. Nucl. Magn. Reson. Spectrosc.* **2011**, *58*, 176.
(35) Schreckenbach, G.; Ziegler, T. *Theor. Chem. Acc.* **1998**, *99*, 71.
(36) Facelli, J. C. *Concepts Magn. Reson.* **2004**, *20A*, 42.
(37) Facelli, J. C.; Grant, D. M.; Michl, J. *Acc. Chem. Res.* **1987**, *20*, 152.
(38) Kaupp, M.; Bühl, M.; Malkin, V. G. *Calculation of NMR and EPR Parameters: Theory and Applications*; Wiley,: 2006.
(39) Vaara, J. *Phys. Chem. Chem. Phys.* **2007**, *9*, 5399.
(40) Facelli, J. C.; Pugmire, R. J.; Grant, D. M. *J. Am. Chem. Soc.* **1996**, *118*, 5488.
(41) Zheng, G.; Wang, L.; Hu, J.; Zhang, X.; Shen, L.; Ye, C.; Webb, G. A. *Magn. Reson. Chem.* **1997**, *35*, 606.
(42) Babinsky, M.; Bouzkova, K.; Pipiska, M.; Novosadova, L.; Marek, R. *J. Phys. Chem. A* **2013**, *117*, 497.
(43) Stueber, D.; Grant, D. M. *J. Am. Chem. Soc.* **2002**, *124*, 10539.
(44) Holmes, S. T.; Dybowski, C. *Solid State Nucl. Magn. Reson.* **2015**, DOI: 10.1016/j.ssnmr.2015.08.004.
(45) Cheeseman, J. R.; Trucks, G. W.; Keith, T. A.; Frisch, M. J. *J. Chem. Phys.* **1996**, *104*, 5497.
(46) Teale, A. M.; Lutnæs, O. B.; Helgaker, T.; Tozer, D. J.; Gauss, J. *J. Chem. Phys.* **2013**, *138*, 024111.
(47) Pickard, C. J.; Mauri, F. *Phys. Rev. B: Condens. Matter Mater. Phys.* **2001**, *63*, 245101.
(48) Broqvist, P.; Alkauskas, A.; Pasquarello, A. *Phys. Rev. B: Condens. Matter Mater. Phys.* **2009**, *80*, 085114.
(49) Perdew, J. P.; Burke, K.; Ernzerhof, M. *Phys. Rev. Lett.* **1996**, *77*, 3865.
(50) Bonhomme, C.; Gervais, C.; Babonneau, F.; Coelho, C.; Pourpoint, F.; Azais, T.; Ashbrook, S. E.; Griffin, J. M.; Yates, J. R.; Mauri, F.; Pickard, C. J. *Chem. Rev.* **2012**, *112*, 5733.
(51) Weber, J.; auf der Gunne, J. S. *Phys. Chem. Chem. Phys.* **2010**, *12*, 583.
(52) Koller, H.; Engelhardt, G.; Kentgens, A. P. M.; Sauer, J. *J. Phys. Chem.* **1994**, *98*, 1544.
(53) Tossell, J. A. *J. Magn. Reson.* **1997**, *127*, 49.
(54) Tossell, J. A. *Chem. Phys. Lett.* **1999**, *303*, 435.
(55) Tossell, J. A. *Phys. Chem. Miner.* **1999**, *27*, 70.
(56) Valerio, G.; Goursot, A.; Vetrivel, R.; Malkina, O.; Malkin, V.; Salahub, D. R. *J. Am. Chem. Soc.* **1998**, *120*, 11426.
(57) Valerio, G.; Goursot, A. *J. Phys. Chem. B* **1999**, *103*, 51.
(58) Orendt, A. M.; Facelli, J. C.; Grant, D. M. *Chem. Phys. Lett.* **1999**, *302*, 499.
(59) Alkan, F.; Dybowski, C. *Phys. Chem. Chem. Phys.* **2014**, *16*, 14298.
(60) Alkan, F.; Dybowski, C. *Phys. Chem. Chem. Phys.* **2015**, *17*, 25014.
(61) Hartman, J. D.; Neubauer, T. J.; Caulkins, B. G.; Mueller, L. J.; Beran, G. J. O. *J. Biomol. NMR* **2015**, 327.
(62) Ditchfield, R. *Mol. Phys.* **1974**, *27*, 789.
(63) Schreckenbach, G.; Ziegler, T. *J. Phys. Chem.* **1995**, *99*, 606.
(64) Sherwood, M. H.; Facelli, J. C.; Alderman, D. W.; Grant, D. M. *J. Am. Chem. Soc.* **1991**, *113*, 750.
(65) Capelli, S. C.; Albinati, A.; Mason, S. A.; Willis, B. T. M. *J. Phys. Chem. A* **2006**, *110*, 11695.
(66) Pausak, S.; Pines, A.; Waugh, J. S. *J. Chem. Phys.* **1973**, *59*, 591.
(67) Prince, E.; Schroeder, L. W.; Rush, J. J. *Acta Crystallogr., Sect. B: Struct. Crystallogr. Cryst. Chem.* **1973**, *29*, 184.
(68) Maliňáková, K.; Novosadová, L.; Lahtinen, M.; Kolehmainen, E.; Brus, J.; Marek, R. *J. Phys. Chem. A* **2010**, *114*, 1985.
(69) Schmalle, H. W.; Hanggi, G.; Dubler, E. *Acta Crystallogr., Sect. C: Cryst. Struct. Commun.* **1988**, *44*, 732.
(70) Sherwood, M. H.; Alderman, D. W.; Grant, D. M. *J. Magn. Reson., Ser. A* **1993**, *104*, 132.
(71) Brown, G. M.; Levy, H. A. *Acta Crystallogr., Sect. B: Struct. Crystallogr. Cryst. Chem.* **1973**, *29*, 790.
(72) Griffin, R. G.; Pines, A.; Pausak, S.; Waugh, J. S. *J. Chem. Phys.* **1975**, *63*, 1267.
(73) Thalladi, V. R.; Nusse, M.; Boese, R. *J. Am. Chem. Soc.* **2000**, *122*, 9227.
(74) Sabine, T. M.; Cox, G. W.; Craven, B. M. *Acta Crystallogr., Sect. B: Struct. Crystallogr. Cryst. Chem.* **1969**, *25*, 2437.
(75) Janes, N.; Ganapathy, S.; Oldfield, E. *J. Magn. Reson.* **1983**, *54*, 111.
(76) Ramanadham, M.; Sikka, S. K.; Chidambaram, R. *Pramana* **1973**, *1*, 247.
(77) Mehring, M.; Becker, J. D. *Phys. Rev. Lett.* **1981**, *47*, 366.
(78) Semmingsen, D.; Hollander, F. J.; Koetzle, T. F. *J. Chem. Phys.* **1977**, *66*, 4405.
(79) Zilm, K. W.; Beeler, A. J.; Grant, D. M.; Michl, J.; Chou, T. C.; Allred, E. L. *J. Am. Chem. Soc.* **1981**, *103*, 2119.
(80) Nijveldt, D.; Vos, A. *Acta Crystallogr., Sect. B: Struct. Sci.* **1988**, *44*, 296.
(81) Zilm, K. W.; Conlin, R. T.; Grant, D. M.; Michl, J. *J. Am. Chem. Soc.* **1980**, *102*, 6672.
(82) van Nes, G. J. H.; Vos, A. *Acta Crystallogr., Sect. B: Struct. Crystallogr. Cryst. Chem.* **1979**, *35*, 2593.
(83) Solum, M. S.; Facelli, J. C.; Gan, Z.; Grant, D. M. *Mol. Phys.* **1988**, *64*, 1031.
(84) Jeffrey, G. A.; Ruble, J. R.; Wingert, L. M.; Yates, J. H.; McMullan, R. K. *J. Am. Chem. Soc.* **1985**, *107*, 6227.
(85) Beeler, A. J.; Orendt, A. M.; Grant, D. M.; Cutts, P. W.; Michl, J.; Zilm, K. W.; Downing, J. W.; Facelli, J. C.; Schindler, M. S.; Kutzelnigg, W. *J. Am. Chem. Soc.* **1984**, *106*, 7672.
(86) McMullan, R. K.; Kvick, A.; Popelier, P. *Acta Crystallogr., Sect. B: Struct. Sci.* **1992**, *48*, 726.
(87) Pines, A.; Waugh, J. S.; Gibby, M. G. *Chem. Phys. Lett.* **1972**, *15*, 373.
(88) Powell, B. M.; Dolling, G.; Torrie, B. H. *Acta Crystallogr., Sect. B: Struct. Crystallogr. Cryst. Chem.* **1982**, *38*, 28.
(89) Alderman, D. W.; Solum, M. S.; Grant, D. M. *J. Chem. Phys.* **1986**, *84*, 3717.
(90) Yokoyama, Y.; Ohashi, Y. *Bull. Chem. Soc. Jpn.* **1999**, *72*, 2183.
(91) Liu, F.; Orendt, A. M.; Alderman, D. W.; Grant, D. M. *J. Am. Chem. Soc.* **1997**, *119*, 8981.
(92) Semmingsen, D. *Acta Chem. Scand.* **1988**, *A42*, 279.
(93) Takegoshi, K.; Naito, A.; McDowell, C. A. *J. Magn. Reson.* **1985**, *65*, 34.
(94) Bolte, M.; Scholtyssik, M. *Acta Crystallogr., Sect. C: Cryst. Struct. Commun.* **1997**, *53*, 1869.
(95) Facelli, J. C.; Orendt, A. M.; Beeler, A. J.; Solum, M. S.; Depke, G.; Malsch, K. D.; Downing, J. W.; Murthy, P. S.; Grant, D. M.; Michl, J. *J. Am. Chem. Soc.* **1985**, *107*, 6749.
(96) Benet-Buchholz, J.; Haumann, T.; Boese, R. *Chem. Commun.* **1998**, 2003.
(97) Orendt, A. M.; Facelli, J. C.; Grant, D. M.; Michl, J.; Walker, F. H.; Dailey, W. P.; Waddell, S. T.; Wiberg, K. B.; Schindler, M.; Kutzelnigg, W. *Theor. Chim. Acta* **1985**, *68*, 421.
(98) Seiler, P. *Helv. Chim. Acta* **1990**, *73*, 1574.

DOI: 10.1021/acs.jctc.5b00752
J. Chem. Theory Comput. XXXX, XXX, XXX−XXX

(99) Tretjak, S. M.; Mitkevich, V. V.; Sukhodub, L. F. *Kristallografiya* **1987**, *32*, 1268.
(100) McClure, R. J.; Craven, B. M. *Acta Crystallogr., Sect. B: Struct. Crystallogr. Cryst. Chem.* **1973**, *B29*, 1234.
(101) Thewalt, U.; Bugg, C. E.; Marsh, R. E. *Acta Crystallogr., Sect. B: Struct. Crystallogr. Cryst. Chem.* **1971**, *B27*, 2358.
(102) Portalone, G.; Bencivenni, L.; Colapietro, M.; Pieretti, A.; Ramondo, F. *Acta Chem. Scand.* **1999**, *53*, 57.
(103) Stewart, R. F. *Acta Crystallogr.* **1967**, *23*, 1102.
(104) Goddard, R.; Heinemann, O.; Kruger, C. *Acta Crystallogr., Sect. C: Cryst. Struct. Commun.* **1997**, *53*, 1846.
(105) Craven, B. M.; McMullan, R. K.; Bell, J. D.; Freeman, H. C. *Acta Crystallogr., Sect. B: Struct. Crystallogr. Cryst. Chem.* **1977**, *33*, 2585.
(106) Hu, J. Z.; Zhou, J. W.; Yang, B. L.; Li, L. Y.; Qiu, J. Q.; Ye, C. H.; Solum, M. S.; Wind, R. A.; Pugmire, R. J.; Grant, D. M. *Solid State Nucl. Magn. Reson.* **1997**, *8*, 129.
(107) Kobayashi, K.; Sato, A.; Sakamoto, S.; Yamaguchi, K. *J. Am. Chem. Soc.* **2003**, *125*, 3035.
(108) Escande, A.; Galigne, J. L. *Acta Crystallogr., Sect. B: Struct. Crystallogr. Cryst. Chem.* **1974**, *30*, 1647.
(109) Penner, G. H.; Bernard, G. M.; Wasylishen, R. E.; Barrett, A.; Curtis, R. D. *J. Org. Chem.* **2003**, *68*, 4258.
(110) Boese, R.; Blaser, D.; Nussbaumer, M.; Krygowski, T. M. *Struct. Chem.* **1992**, *3*, 363.
(111) Wasylishen, R. E.; Penner, G. H.; Power, W. P.; Curtis, R. D. *J. Am. Chem. Soc.* **1989**, *111*, 6082.
(112) Gieren, A.; Hubner, T.; Ruizperez, C. *Chem. Zeit.* **1986**, *110*, 73.
(113) Crawford, S.; Kirchner, M. T.; Blaser, D.; Boese, R.; David, W. I. F.; Dawson, A.; Gehrke, A.; Ibberson, R. M.; Marshall, W. G.; Parsons, S.; Yamamuro, O. *Angew. Chem., Int. Ed.* **2009**, *48*, 755.
(114) Marsh, R. E.; Kapon, M.; Hu, S. Z.; Herbstein, F. H. *Acta Crystallogr., Sect. B: Struct. Sci.* **2002**, *58*, 62.
(115) Kaplan, S.; Pines, A.; Griffin, R. G.; Waugh, J. S. *Chem. Phys. Lett.* **1974**, *25*, 78.
(116) Enjalbert, R.; Galy, J. *Acta Crystallogr., Sect. B: Struct. Sci.* **2002**, *58*, 1005.
(117) Sardashti, M.; Maciel, G. E. *J. Phys. Chem.* **1988**, *92*, 4620.
(118) Guth, H.; Heger, G.; Druck, U. *Z. Kristallogr. - Cryst. Mater.* **1982**, *159*, 185.
(119) Curtis, R. D.; Hilborn, J. W.; Wu, G.; Lumsden, M. D.; Wasylishen, R. E.; Pincock, J. A. *J. Phys. Chem.* **1993**, *97*, 1856.
(120) Mostad, A.; Romming, C. *Acta Chem. Scand.* **1971**, *25*, 3561.
(121) Wasylishen, R. E.; Power, W. P.; Penner, G. H.; Curtis, R. D. *Can. J. Chem.* **1989**, *67*, 1219.
(122) Harada, J.; Ogawa, K.; Tomoda, S. *Acta Crystallogr., Sect. B: Struct. Sci.* **1997**, *53*, 662.
(123) Harbison, G. S.; Kye, Y.-S.; Penner, G. H.; Grandin, M.; Monette, M. *J. Phys. Chem. B* **2002**, *106*, 10285.
(124) Kanda, F. A.; King, A. J. *J. Am. Chem. Soc.* **1951**, *73*, 2315.
(125) Raber, H.; Mehring, M. *Chem. Phys.* **1977**, *26*, 123.
(126) Thalladi, V. R.; Weiss, H. C.; Blaser, D.; Boese, R.; Nangia, A.; Desiraju, G. R. *J. Am. Chem. Soc.* **1998**, *120*, 8702.
(127) Kirchner, M. T.; Blaser, D.; Boese, R.; Thakur, T. S.; Desiraju, G. R. *Acta Crystallogr., Sect. E: Struct. Rep. Online* **2009**, *65*, O2668.
(128) Molski, M. J.; Mollenhauer, D.; Gohr, S.; Paulus, B.; Khanfar, M. A.; Shorafa, H.; Strauss, S. H.; Seppelt, K. *Chem. - Eur. J.* **2012**, *18*, 6644.
(129) Mehring, M.; Griffin, R. G.; Waugh, J. S. *J. Chem. Phys.* **1971**, *55*, 746.
(130) Shorafa, H.; Mollenhauer, D.; Paulus, B.; Seppelt, K. *Angew. Chem., Int. Ed.* **2009**, *48*, 5845.
(131) Harris, R. K.; Jackson, P.; Nesbitt, G. J. *J. Magn. Reson.* **1989**, *85*, 294.
(132) Akhmed, N. A. *Zh. Strukt. Khim.* **1973**, *14*, 573.
(133) Hathwar, V. R.; Thakur, T. S.; Dubey, R.; Pavan, M. S.; Row, T. N. G.; Desiraju, G. R. *J. Phys. Chem. A* **2011**, *115*, 12852.
(134) Kubota, M.; Ohba, S. *Acta Crystallogr., Sect. B: Struct. Sci.* **1992**, *48*, 849.
(135) Halstead, T. K.; Spiess, H. W.; Haeberlen, U. *Mol. Phys.* **1976**, *31*, 1569.
(136) Lemee, M. H.; Toupet, L.; Delugeard, Y.; Messager, J. C.; Cailleau, H. *Acta Crystallogr., Sect. B: Struct. Sci.* **1987**, *43*, 466.
(137) Oswald, I. D. H.; Allan, D. R.; Motherwell, W. D. S.; Parsons, S. *Acta Crystallogr., Sect. B: Struct. Sci.* **2005**, *61*, 69.
(138) Ridout, J.; Probert, M. R. *Cryst. Growth Des.* **2013**, *13*, 1943.
(139) Hagen, K.; Nicholson, D. G.; Saethre, L. J. *Acta Crystallogr., Sect. C: Cryst. Struct. Commun.* **1987**, *43*, 1959.
(140) Guo, Q. Z.; Sears, R. E. J.; Campbell, R. D. *J. Chem. Phys.* **1984**, *81*, 5214.
(141) Cockcroft, J. K.; Fitch, A. N. *Z. Kristallogr.* **1994**, *209*, 488.
(142) Robert, J. B.; Wiesenfeld, L. *Mol. Phys.* **1981**, *44*, 319.
(143) Hursthouse, M. B.; Hart, F. A.; Backer-Dirkis, J. D. J. Private Communication (CCDC 679505).
(144) Brock, C. P.; Schweizer, W. B.; Dunitz, J. D. *J. Am. Chem. Soc.* **1985**, *107*, 6964.
(145) Grimmer, A. R.; Muller, D. *Z. Chem.* **1976**, *16*, 496.
(146) Olie, K. *Acta Crystallogr., Sect. B: Struct. Crystallogr. Cryst. Chem.* **1971**, *B27*, 1459.
(147) Shenderovich, I. G. *J. Phys. Chem. C* **2013**, *117*, 26689.
(148) Dornhaus, F.; Bolte, M.; Lerner, H. W.; Wagner, M. *Eur. J. Inorg. Chem.* **2006**, *2006*, 5138.
(149) Tasker, P.; Coventry, D.; Parsons, S.; Messenger, D. Private Communication (CCDC 276835).
(150) Gee, M.; Wasylishen, R. E.; Eichele, K.; Britten, J. F. *J. Phys. Chem. A* **2000**, *104*, 4598.
(151) Lee, J. D.; Goodacre, G. W. *Acta Crystallogr., Sect. B: Struct. Crystallogr. Cryst. Chem.* **1971**, *B27*, 302.
(152) Eichele, K.; Wu, G.; Wasylishen, R. E.; Britten, J. F. *J. Phys. Chem.* **1995**, *99*, 1030.
(153) Cogne, A.; Grand, A.; Laugier, J.; Robert, J. B.; Wiesenfeld, L. *J. Am. Chem. Soc.* **1980**, *102*, 2238.
(154) Herzfeld, J.; Griffin, R. G.; Haberkorn, R. A. *Biochemistry* **1978**, *17*, 2711.
(155) Wilson, C. C.; Shankland, K.; Shankland, N. *Z. Kristallogr. - Cryst. Mater.* **2001**, *216*, 303.
(156) Reuter, H.; Reichelt, M. *Acta Crystallogr., Sect. E: Struct. Rep. Online* **2014**, *70*, o353.
(157) Eichele, K.; Wasylishen, R. E.; Kessler, J. M.; Solujic, L.; Nelson, J. H. *Inorg. Chem.* **1996**, *35*, 3904.
(158) Decken, A. Private Communication (CCDC 254271).
(159) Wu, G.; Wasylishen, R. E. *Solid State Nucl. Magn. Reson.* **1995**, *4*, 47.
(160) Kaiser, V.; Menzel, F. *Z. Kristallogr. - Cryst. Mater.* **1993**, *206*, 279.
(161) Kempe, R.; Sieler, J.; Beckmann, H.; Ohms, G. *Z. Kristallogr.* **1992**, *202*, 159.
(162) Gudat, D.; Hoffbauer, W.; Niecke, E.; Schoeller, W. W.; Fleischer, U.; Kutzelnigg, W. *J. Am. Chem. Soc.* **1994**, *116*, 7325.
(163) Nieger, N.; Cartner-Winkhaus, C.; Niecke, E. Private Communication (CCDC 174707).
(164) Chernega, A. N.; Korkin, A. A.; Aksinenko, N. E.; Ruban, A. V.; Romanenko, V. D. *Zh. Obshch. Khim.* **1990**, *60*, 2462.
(165) Penner, G. H.; Wasylishen, R. E. *Can. J. Chem.* **1989**, *67*, 1909.
(166) Davies, J. A.; Dutremez, S.; Pinkerton, A. A. *Inorg. Chem.* **1991**, *30*, 2380.
(167) Barra, A. L.; Robert, J. B. *Chem. Phys. Lett.* **1987**, *136*, 224.
(168) Marinetti, A.; Mathey, F.; Fischer, J.; Mitschler, A. *J. Chem. Soc., Chem. Commun.* **1984**, 45.
(169) Barra, A. L.; Robert, J. B. *Chem. Phys. Lett.* **1988**, *149*, 363.
(170) Appel, R.; Gaitzsch, T.; Knoch, F.; Lenz, G. *Chem. Ber.* **1986**, *119*, 1977.
(171) Liu, F.; Phung, C. G.; Alderman, D. W.; Grant, D. M. *J. Am. Chem. Soc.* **1996**, *118*, 10629.
(172) Harper, J. K.; Iuliucci, R.; Gruber, M.; Kalakewich, K. *CrystEngComm* **2013**, *15*, 8693.

DOI: 10.1021/acs.jctc.5b00752
J. Chem. Theory Comput. XXXX, XXX, XXX−XXX

(173) Clark, S. J.; Segall, M. D.; Pickard, C. J.; Hasnip, P. J.; Probert, M. J.; Refson, K.; Payne, M. C. *Z. Kristallogr. - Cryst. Mater.* **2005**, *220*, 567.
(174) Frisch, M. J.; Trucks, G. W.; Schlegel, H. B.; Scuseria, G. E.; Robb, M. A.; Cheeseman, J. R.; Scalmani, G.; Barone, V.; Mennucci, B.; Petersson, G. A.; Nakatsuji, H.; Caricato, M.; Li, X.; Hratchian, H. P.; Izmaylov, A. F.; Bloino, J.; Zheng, G.; Sonnenberg, J. L.; Hada, M.; Ehara, M.; Toyota, K.; Fukuda, R.; Hasegawa, J.; Ishida, M.; Nakajima, T.; Honda, Y.; Kitao, O.; Nakai, H.; Vreven, T.; Montgomery, J. A.; Peralta, J. E.; Ogliaro, F.; Bearpark, M.; Heyd, J. J.; Brothers, E.; Kudin, K. N.; Staroverov, V. N.; Kobayashi, R.; Normand, J.; Raghavachari, K.; Rendell, A.; Burant, J. C.; Iyengar, S. S.; Tomasi, J.; Cossi, M.; Rega, N.; Millam, J. M.; Klene, M.; Knox, J. E.; Cross, J. B.; Bakken, V.; Adamo, C.; Jaramillo, J.; Gomperts, R.; Stratmann, R. E.; Yazyev, O.; Austin, A. J.; Cammi, R.; Pomelli, C.; Ochterski, J. W.; Martin, R. L.; Morokuma, K.; Zakrzewski, V. G.; Voth, G. A.; Salvador, P.; Dannenberg, J. J.; Dapprich, S.; Daniels, A. D.; Farkas; Foresman, J. B.; Ortiz, J. V.; Cioslowski, J.; Fox, D. J. Wallingford C. T. *Gaussian 09*; 2009.
(175) Dunning, T. H. *J. Chem. Phys.* **1989**, *90*, 1007.
(176) Woon, D. E.; Dunning, T. H. *J. Chem. Phys.* **1993**, *98*, 1358.
(177) Perdew, J. P.; Wang, Y. *Phys. Rev. B: Condens. Matter Mater. Phys.* **1992**, *45*, 13244.
(178) Becke, A. D. *J. Chem. Phys.* **1993**, *98*, 1372.
(179) Adamo, C.; Barone, V. *J. Chem. Phys.* **1999**, *110*, 6158.
(180) Tao, J. M.; Perdew, J. P.; Staroverov, V. N.; Scuseria, G. E. *Phys. Rev. Lett.* **2003**, *91*, 146401.
(181) Srebro, M.; Autschbach, J. *Chem. - Eur. J.* **2013**, *19*, 12018.
(182) Dracinsky, M.; Hodgkinson, P. *CrystEngComm* **2013**, *15*, 8705.
(183) Jensen, F. *J. Chem. Theory Comput.* **2006**, *2*, 1360.
(184) Jensen, F. *J. Chem. Theory Comput.* **2008**, *4*, 719.
(185) Kupka, T.; Ruscic, B.; Botto, R. E. *J. Phys. Chem. A* **2002**, *106*, 10396.
(186) Kupka, T.; Ruscic, B.; Botto, R. E. *Solid State Nucl. Magn. Reson.* **2003**, *23*, 145.
(187) Moon, S.; Case, D. A. *J. Comput. Chem.* **2006**, *27*, 825.
(188) Sefzik, T. H.; Fidler, J. M.; Iuliucci, R. J.; Facelli, J. C. *Magn. Reson. Chem.* **2006**, *44*, 390.
(189) Chesnut, D. B.; Moore, K. D. *J. Comput. Chem.* **1989**, *10*, 648.
(190) Chesnut, D. B.; Rusiloski, B. E.; Moore, K. D.; Egolf, D. A. *J. Comput. Chem.* **1993**, *14*, 1364.
(191) Zurek, E.; Pickard, C. J.; Walczak, B.; Autschbach, J. *J. Phys. Chem. A* **2006**, *110*, 11995.
(192) Zurek, E.; Pickard, C. J.; Autschbach, J. *J. Am. Chem. Soc.* **2007**, *129*, 4430.
(193) O'Dell, L. A.; Schurko, R. W.; Harris, K. J.; Autschbach, J.; Ratcliffe, C. I. *J. Am. Chem. Soc.* **2011**, *133*, 527.
(194) Jensen, F. *J. Chem. Theory Comput.* **2015**, *11*, 132.
(195) Rauhut, G.; Puyear, S.; Wolinski, K.; Pulay, P. *J. Phys. Chem.* **1996**, *100*, 6310.
(196) Laskowski, R.; Blaha, P. *J. Phys. Chem. C* **2015**, *119*, 731.
(197) Hill, D. E.; Vasdev, N.; Holland, J. P. *Comput. Theor. Chem.* **2015**, *1051*, 161.
(198) Keal, T. W.; Tozer, D. J.; Helgaker, T. *Chem. Phys. Lett.* **2004**, *391*, 374.
(199) Keal, T. W.; Helgaker, T.; Sałek, P.; Tozer, D. J. *Chem. Phys. Lett.* **2006**, *425*, 163.
(200) San Fabian, J.; de la Vega, J. M. G.; San Fabian, E. *J. Chem. Theory Comput.* **2014**, *10*, 4938.
(201) Zhao, Y.; Truhlar, D. G. *J. Phys. Chem. A* **2008**, *112*, 6794.
(202) Sefzik, T. H.; Turco, D.; Iuliucci, R. J.; Facelli, J. C. *J. Phys. Chem. A* **2005**, *109*, 1180.
(203) Czernek, J.; Pawlak, T.; Potrzebowski, M. J. *Chem. Phys. Lett.* **2012**, *527*, 31.
(204) Czernek, J.; Pawlak, T.; Potrzebowski, M. J.; Brus, J. *Chem. Phys. Lett.* **2013**, *555*, 135.
(205) Pawlak, T.; Jaworska, M.; Potrzebowski, M. J. *Phys. Chem. Chem. Phys.* **2013**, *15*, 3137.
(206) Jameson, A. K.; Jameson, C. J. *Chem. Phys. Lett.* **1987**, *134*, 461.
(207) Jameson, C. J.; Jameson, A. K.; Oppusunggu, D.; Wille, S.; Burrell, P. M.; Mason, J. *J. Chem. Phys.* **1981**, *74*, 81.
(208) Jameson, C. J.; Jameson, A. K.; Burrell, P. M. *J. Chem. Phys.* **1980**, *73*, 6013.
(209) Jameson, C. J.; De Dios, A.; Jameson, A. K. *Chem. Phys. Lett.* **1990**, *167*, 575.

DOI: 10.1021/acs.jctc.5b00752
J. Chem. Theory Comput. XXXX, XXX, XXX−XXX